

Original Research

Study of Shape Memory Alloy Fibers for the Development of Artificial Myocardium

IOANNIS A. HASSOULAS¹, VLASSIOS S. LADOPOULOS², PARIS-DIMITRIOS K. KALOGERAKOS¹

¹Cardiac Surgery Department, University of Crete, Faculty of Medicine, ²Foundation for Research and Technology Hellas, Institute of Electronic Structure and Laser, Heraklion, Crete, Greece

Key words: **Heart failure, cardiac compression, artificial myocardium, SMA (shape memory alloy) fibers, no blood contacting artificial surface, current shaping.**

Introduction: Circulatory support devices are employed to treat heart failure. Such a device could be made from shape memory alloy (SMA) fibers. These Ni-Ti fibers contract when electric current flows through them, thus resembling artificial muscles. An artificial myocardium device made from SMA fibers can directly compress the epicardial surface of a failing heart, thus contributing to the pumping action. Unlike modern mechanical circulatory support devices, there is no blood-contacting surface to provoke thromboembolism, hemorrhage, inflammatory response or hemolysis.

Methods: The experimental setup permitted a detailed study of a sample SMA fiber with great accuracy while the ambient temperature was controlled to resemble that of the human body. The current profile through the fiber was controlled (current shaping, CS) by a microcontroller and a portable computer.

Results: Parameters such as strain, contraction and relaxation velocities and the effect of ambient temperature were measured. The contraction and relaxation velocities were measured after applying various effective currents. It was found that the contraction velocity could be manipulated to reach that of the healthy myocardium through CS. On the other hand, the relaxation velocity was independent of the contraction velocity.

Conclusions: A cardiac assist device can be made from SMA fibers. More studies need to be conducted in this direction.

Manuscript received:

April 21, 2009;

Accepted:

December 14, 2009.

Address:

Paris-Dimitrios
K. Kalogerakos

Foundation for Research
and Technology Hellas
Institute of Electronic
Structure and Laser
Heraklion, Crete, Greece
e-mail: pariskal@yahoo.gr,
vlad@iesl.forth.gr

Hart failure is a major cause of mortality worldwide. A widely used method of treatment for heart failure includes the implantation of mechanical circulatory support (MCS) devices. A common problem of MCS devices is the artificial surface in contact with blood that causes thromboembolism, hemorrhage, inflammatory response and hemolysis.¹⁻³ Other frequent disadvantages of these devices are their large size, the mechanical malfunctions that can occur⁴ and their energy demands. A method of MCS that might possibly avoid these drawbacks is the application of direct cardiac compression (DCC) to the epicardial surface of the failing heart. This pressure assists the myocardial movement and the device thus contributes to the pumping

action of the heart.⁵⁻⁸ The reasonable concern about jeopardizing the myocardial perfusion, given that the coronary arteries lie right under the epicardium, has been proven unjustified. On the contrary, during DCC myocardial perfusion increases.^{6,9}

Two other methods of treating heart failure that utilize wrapping around the heart are cardiomyoplasty with the *latissimus dorsi* muscle and the passive constraint of heart dilation using a net (Acorn Cor-Cap). The main disadvantages of cardiomyoplasty are atrophy, lipoid degeneration, and fatigue of the *latissimus dorsi* muscle and its adhesion to the heart. Nevertheless cardiomyoplasty could be used as a bridge to transplantation.¹⁰ On the other hand, the Acorn CorCap does not contribute to the pumping action of the heart, but instead re-

duces the wall stress and promotes reverse remodeling. The use of the Acorn CorCap can be combined with a mitral annuloplasty procedure with good results.¹¹

The development of DCC devices without these drawbacks can be based on the use of shape memory alloy (SMA) fibers. The property of these fibers to contract could enable them to compress and thus assist a failing heart. An artificial myocardium developed from SMA fibers would be characterized by the absence of any blood-contacting artificial surface, pulsatile flow, the restraint of heart dilatation, the improvement of myocardial perfusion, the possible scenario of heart recovery,^{2,12} a small size, and the reliability of these fibers to contract and relax over long periods of time.

SMA fibers contract because of a change in their internal crystalline structure when their temperature increases, as is the case when an electrical current flows through them. When the current stops flowing the fibers begin to cool and gradually return to their original size after some hysteresis (Figure 1).¹³ A thorough study of the properties of SMA fibers is essential in order to methodically develop an artificial myocardium. For this purpose, the following experiment was carried out in our laboratory at the Foundation for Research and Technology (FORTH).

Methods

We obtained SMA fibers with diameters of 50, 100 and 150 μm . The study of these samples was conducted in a laboratory setup that could determine

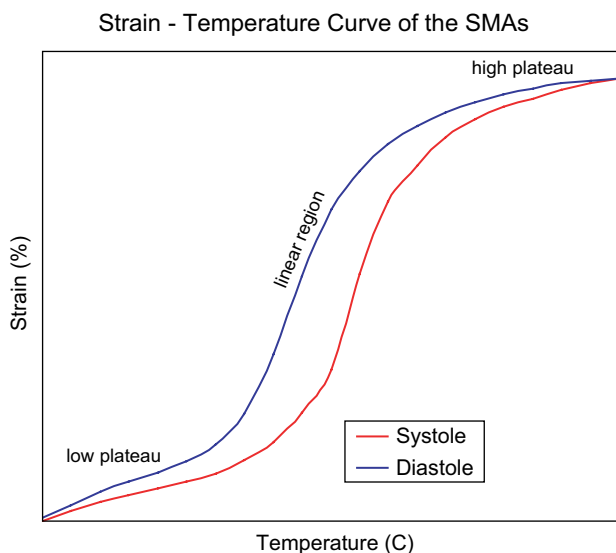


Figure 1. Strain-temperature curve of the shape memory alloys.

with great accuracy the strain and the produced force of these fibers, as well as the impact of various ambient temperatures and electrical current flows.

The central apparatus (Figure 2) of this experiment consisted of a metallic platform (8 × 19 cm) with a perpendicular stand that held a load cell. The SMA fiber under investigation was suspended from a hook on the weighing side of the load cell. The other end of the SMA fiber was partially wrapped around a cylinder that carried a mirror along its axis. This cylinder could rotate freely between two stands and had a hook for hanging weights in series with the fiber. When the fiber, which was fixed to the immovable load cell and the revolving cylinder, contracted, the cylinder rotated and the weight was lifted up. The mirror rotated with the cylinder and reflected a laser beam coming from a laser-pointer placed near the load cell. The reflected laser beam pointed at a metallic arc (Figure 3) placed 2 m away. This arc was graduated in 1 cm intervals and had 13 photodiodes (PD). The length of the arc of the laser beam's deflection, DL' , corresponded to a shortening, DL , of the SMA fiber according to the following equation, in

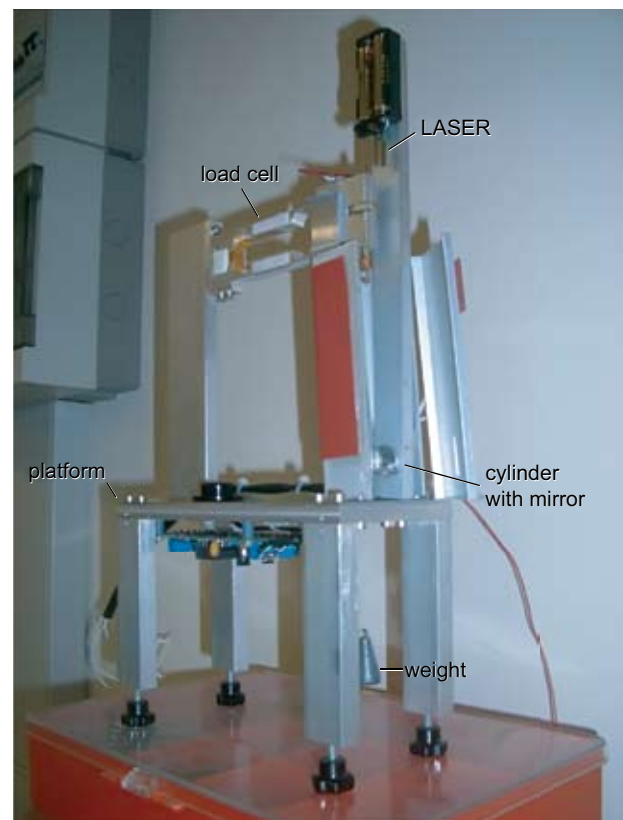


Figure 2. Central apparatus. The fiber is very thin and cannot be seen.



Figure 3. The metallic arc 2 m away from the central apparatus.

which r is the radius of the cylinder and r' the distance between the mirror and the metallic arc.

$$\text{Eq. 1. } DL = (r/2r') \times DL' \text{ (Figure 4).}$$

This design allowed the measurement of the fiber's strain with great accuracy, since every change was magnified 528 times ($2r'/r$). The PDs were connected to an oscilloscope that measured the time interval between the excitation of these PDs because of the laser beam movement. In this way the velocity of the laser beam's rotation could be measured and hence the velocity (V) of the fiber contracting or expanding:

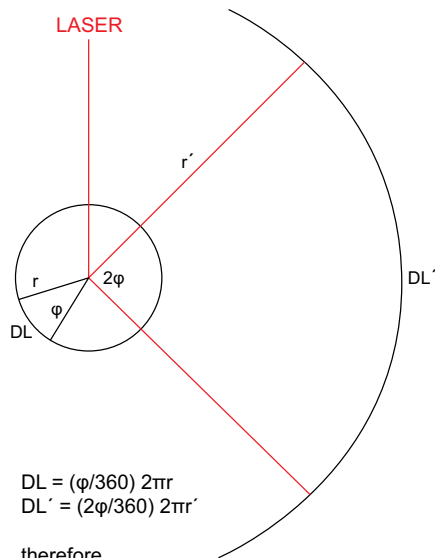
$$\text{Eq. 2. } V = (r/2r') (\Delta DL'/t),$$

where t is the time interval and $\Delta DL'$ is the change in DL' .

The fiber was surrounded by an aluminum case with self adhesive heat pads to simulate ambient temperature. The resistive heat pads were connected to a thermostat that controlled the heating of the fiber space to given temperatures and enabled us to simulate body temperatures.

If the initial length of the fiber is L_0 , the strain equation is:

$$\text{Eq. 3. } s = (DL/L_0) \times 100\%.$$



$$DL = (\varphi/360) 2\pi r$$

$$DL' = (2\varphi/360) 2\pi r'$$

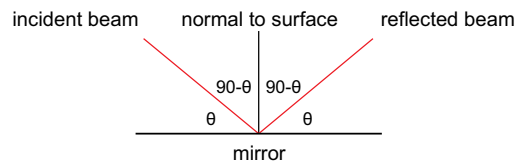
therefore

$$DL = (r/2r') DL'$$

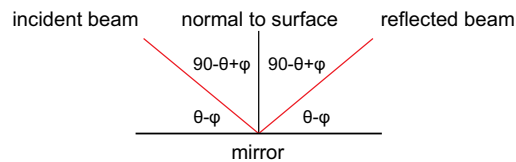
dividing this equation by the time t

$$V = (r/2r') (DL'/t)$$

V is the velocity of the fiber



When the mirror rotates φ degrees, the reflected beam rotates 2φ degrees. The new angle between the beam and the mirror is $\theta-\varphi$.



So the angle between the incident beam and the reflected beam is increased 2φ degrees. Before the rotation of the mirror it was $2(90-\theta) = 180-2\theta$ and after the rotation it is $2(90-\theta+\varphi) = 180-2\theta+2\varphi$

Figure 4. Design of the experiment.

The electrical current that caused the contraction of the SMA fiber was provided by a current source that was manually controlled and could provide a current flow from 0 to 200 mA. This value was the I_{max} . The current flowed through a pulse width modulation controller and the effective current I_{ef} varied between 0 and I_{max} . The controller received commands from a microcontroller, which in turn received commands from a portable computer. The controller's program had the following variables, which were set by the computer:

- BPM (beats per minute).
- $Cr_{d_{on}}$ (maximum duration of current flow $\leq Cr_{d_{on}}$ max which is automatically calculated from the BPM) in ms.
- P_{od} (Peak On Duration $\leq Cr_{d_{on}}$) in ms.
- P_{dc} (Peak Duty Cycle) from 0 to 99%.
- Hld (Hold Duty Cycle from 0 to 99%, its duration is automatically calculated as $Cr_{d_{on}} - P_{od}$)

The duty cycle (DC) is the fraction of time that a system or device is in the active state.

Eq. 4. $DC = t_{on} / (t_{on} + t_{off})$ (Figure 5).

The effective current I_{ef} after the controller is thus:

Eq. 5. $I_{ef} = I_{max} \times DC$.

This enabled the dynamic control of the current flow through the fiber during its contraction and consequently its velocity. Thus, the current curve could look like Figure 6, in which two steps can be seen. The height of each step is a linear correlation of the respective DC. The steps could be more than two and each height (current intensity) and width (time duration) could be modified. This process of current modification we call "current shaping"; it permits the exact control of the fiber's contracting speed. Using a voltage source and a current meter the resistance of

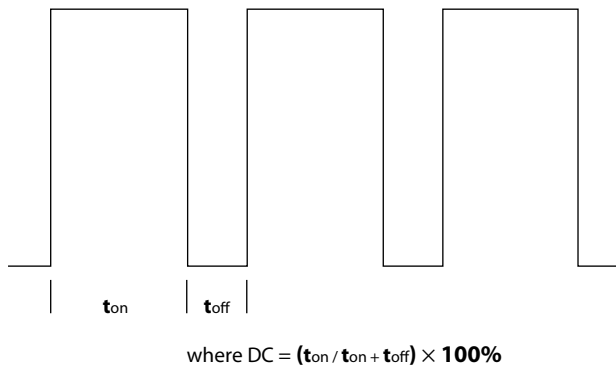


Figure 5. Pulse width modulation. DC – on duty cycle; t – time.

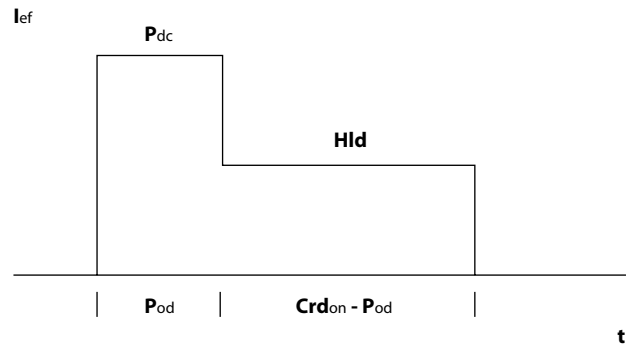


Figure 6. Current shaping. $Cr_{d_{on}}$ – duration of current flow; Hld – hold duty cycle; P_{dc} – peak on duty cycle; P_{od} – peak on duration.

the SMA fiber could be derived, in order to study its relationship to strain.

Results

The fiber under study had a diameter of 50 μm . The contraction and relaxation cycles of the fiber at different ambient temperatures are shown in Figures 7 and 8. Figures 9 and 10 show the relation between ambient temperature and the fiber's contraction and relaxation curves, respectively. The effect of increasing I_{max} to 95 mA can be seen in Figures 11 and 12. The velocities of the fiber's response are shown in Figures 13 to 15, for different values of I_{max} . Figure 16 shows the relation between the fiber's zero-current strain and variations in temperature.

It appears, at least for the 50 μm fiber, that at an ambient temperature of 37 $^{\circ}C$ the fiber enters almost immediately into the linear region of its curve and the low plateau is considerably reduced. In the low plateau the effect of the current flow on the fiber's strain is small. The more the temperature was increased, the more the low plateau was shortened. It appears that at body temperature the SMA fibers need less energy to operate than at room temperature. Figure 9 shows that for a given DC, for instance $DC=50$, at 23 $^{\circ}C$ the DL is 76 cm, at 32.5 $^{\circ}C$ the DL is 153 cm and at 42 $^{\circ}C$ the DL is 166.5 cm, meaning that the same DC, i.e. the same amount of energy, produces a bigger strain as the ambient temperature of the fiber rises. Contrarily, the final strain of the fiber was slightly reduced as the ambient temperature was increased, hopefully without any serious consequences. In addition, the low plateau shortens when the intensity of the current flow increases (Figures 8 & 12).

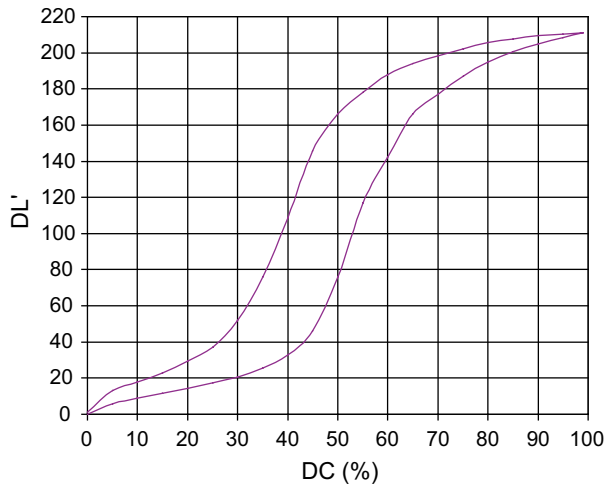


Figure 7. Contraction and relaxation cycle of the fiber: diameter=50 μm , $I_{\text{max}}=80\text{ mA}$, load=21 grf, $t=23^\circ\text{C}$, $s=3.8\%$.

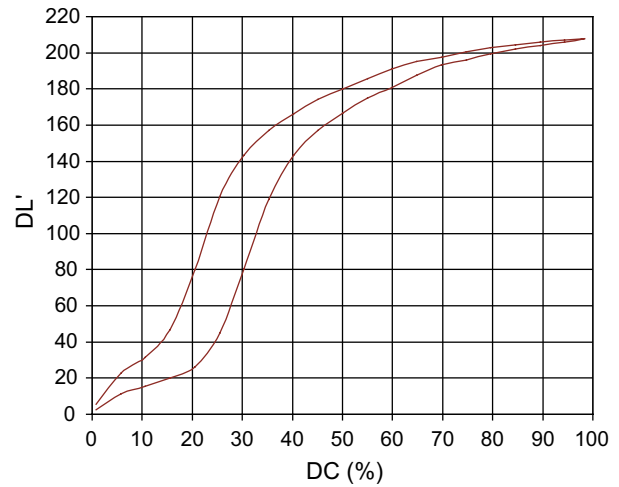


Figure 8. Contraction and relaxation cycle of the fiber: diameter=50 μm , $I_{\text{max}}=80\text{ mA}$, load=21 grf, $t=42^\circ\text{C}$, $s=3.76\%$.

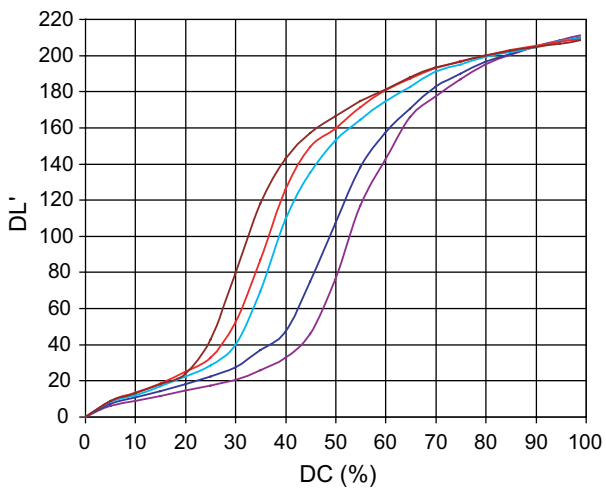


Figure 9. Contraction curves of the fiber at different ambient temperatures. The curves from left to right correspond to temperatures of 42, 37, 32.5, 28 and 23°C . An increase in the temperature causes a leftward shift in the curves and a decrease in final strain.

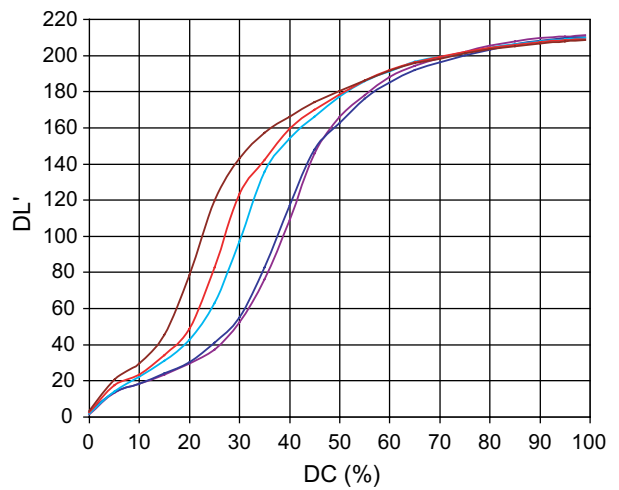


Figure 10. Relaxation curves of the fiber at different ambient temperatures. The curves from left to right correspond to temperatures of 42, 37, 32.5, 28 and 23°C .

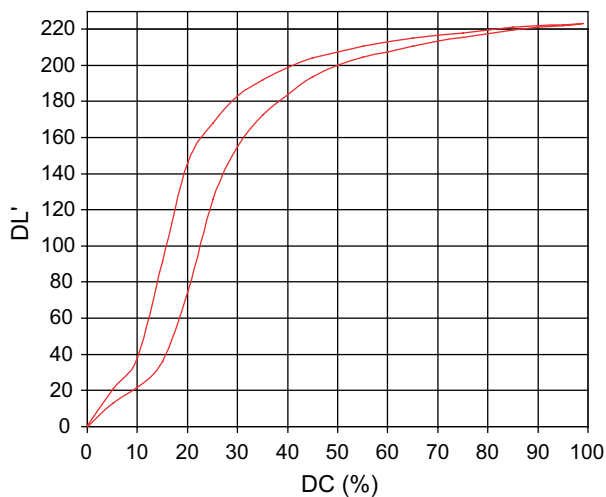


Figure 11. Contraction and relaxation cycle of the fiber: diameter=50 μm , $I_{\text{max}}=95\text{ mA}$, load=21 grf, $t=37^\circ\text{C}$, $s=4.02\%$.

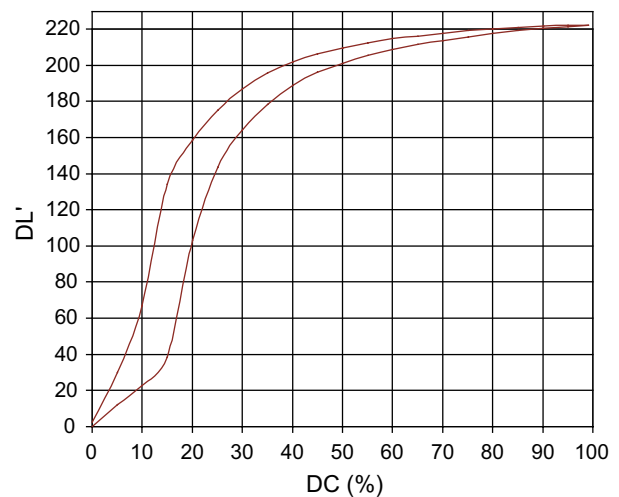


Figure 12. Contraction and relaxation cycle of the fiber: diameter=50 μm , $I_{\text{max}}=95\text{ mA}$, load=21 grf, $t=42^\circ\text{C}$, $s=4\%$.

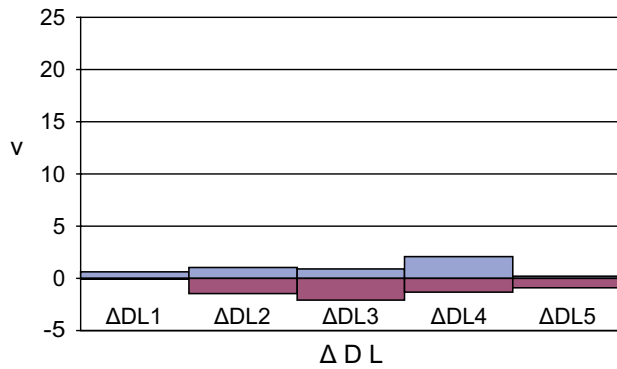


Figure 13. Velocities of the fiber's response, in cm/s: diameter=50 μ m, I_{max} =85 mA, load=21 grf, t =21.8°C. The positive values refer to the contraction and the negative to relaxation.

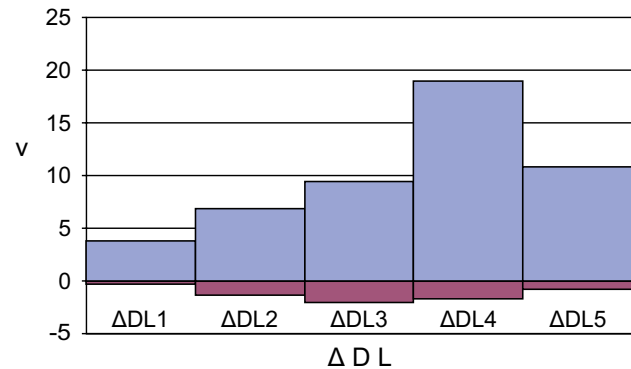


Figure 14. Velocities of the fiber's response, in cm/s: diameter=50 μ m, I_{max} =150 mA, load=21 grf, t =21.8°C. The positive values refer to the contraction and the negative to relaxation.

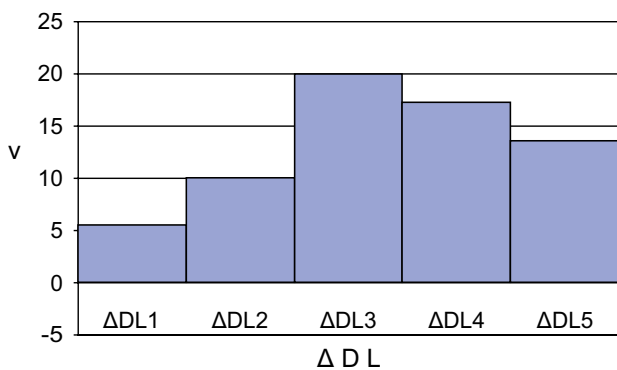


Figure 15. Velocities of the fiber's response, in cm/s: diameter=50 μ m, I_{max} =172 mA, current shaping (100 ms-99%, 200 ms-30%), load=21 grf, t =21.8°C.

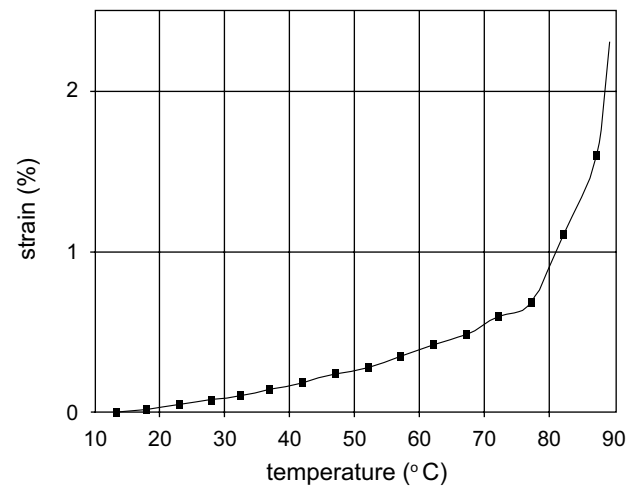


Figure 16. Strain versus temperature (13.5-89°C).

Figures 13 and 14 reveal that an increase of I_{max} causes an increase in the contraction velocity, whereas the relaxation velocity remains unaffected. The use of current shaping, as shown in Figure 15, proves that controlling the fiber's contraction velocity is feasible and that the SMA fibers can contract with a velocity similar to that of healthy myocardium. In a healthy heart the maximum myocardial velocity on the heart's long axis is around 12.5 cm/s, while the mean value is smaller, around 5 cm/s.¹⁴ The maximum velocity of circumferential fiber shortening in normal left ventricular function is 1.58 ± 0.23 circ/s (circ – circumference), whereas in pathological left ventricular function it is 0.91 ± 0.09 circ/s¹⁵ or even less.¹⁶ The mean velocity of circumferential fiber shortening is 1.45 ± 0.08 circ/s.¹⁵ The maximum velocity of the cardiac wall has been shown to shift towards the late systole under some pathological conditions.¹⁵ By using current shaping, an artificial myocardium's contraction velocity can be precisely controlled and the artificial

myocardium could assist the failing heart in early systole when the cardiac wall normally obtains its greatest velocity. In this manner, the pathological movement of the cardiac wall could be ameliorated.

It is apparent that the SMA fibers mainly shorten when operated in the linear region of their curve, so it may be unnecessary to be push them into the high plateau region for four reasons. First, the energy consumption in this saturation region is proportionally much greater than in the linear region and produces less strain per unit current. Second, it appears preferable to decrease the intensity of the current flow before entrance to the high plateau, in order to allow the fibers to relax faster. Third, the fibers' strain at the end of the linear region of their curve is very close to their final strain and it seems that a failing heart could really be assisted even with this very small reduction of the fibers' strain. And finally, if the fibers

do not operate at the limit of their strain capacity, their lifespan is increased.

Discussion

The strain of these SMA fibers is about 4%, whereas the circumference at the base of the heart reduces by about 9.5% during systole.¹⁷ This discrepancy is not discouraging because even this 4% would be beneficial to a failing heart. The force that these fibers produce is great. According to the manufacturer, the fibers with diameter 50, 100 and 150 μm produce forces of 18, 70 and 150 g, respectively. The force of the artificial myocardium device will be proportional to the number of fibers and their thickness. The work produced by the artificial myocardium will be added to the weak heart's work, contributing to the pumping action and reducing myocardial oxygen consumption (Figure 17).¹⁸

An increase in the environmental temperature augments the fibers' temperature and this is manifested as an increase in the fibers' intermediate strain.

The environmental temperature of the SMA fibers will increase when the fibers are placed inside the body and it will change every time the body temperature changes, as in fever. However, as Figure 16 demonstrates, these temperature changes have a negligible effect on the fibers' strain. Moreover, a temperature rise decreases the energy demands of the fibers. These minimal increases in the fibers' strain could never pose a threat of cardiac tamponade. In surgical implantation of the Acorn CorCap the cardiac diameter can be reduced by 5 to 10%, so changes in the fibers' strain due to the above mentioned temperature variations are insignificant.

The exact length of the fibers and every aspect of their operation must be accurately controlled by an algorithm. The electrical activity of the heart, the cardiac output and the hemoglobin oxygen saturation could provide the input information for this algorithm. It is obvious that the contraction of the artificial myocardium must be synchronized with the patient's heart. This could be achieved by monitoring the cardiac electrical activity in the same manner as

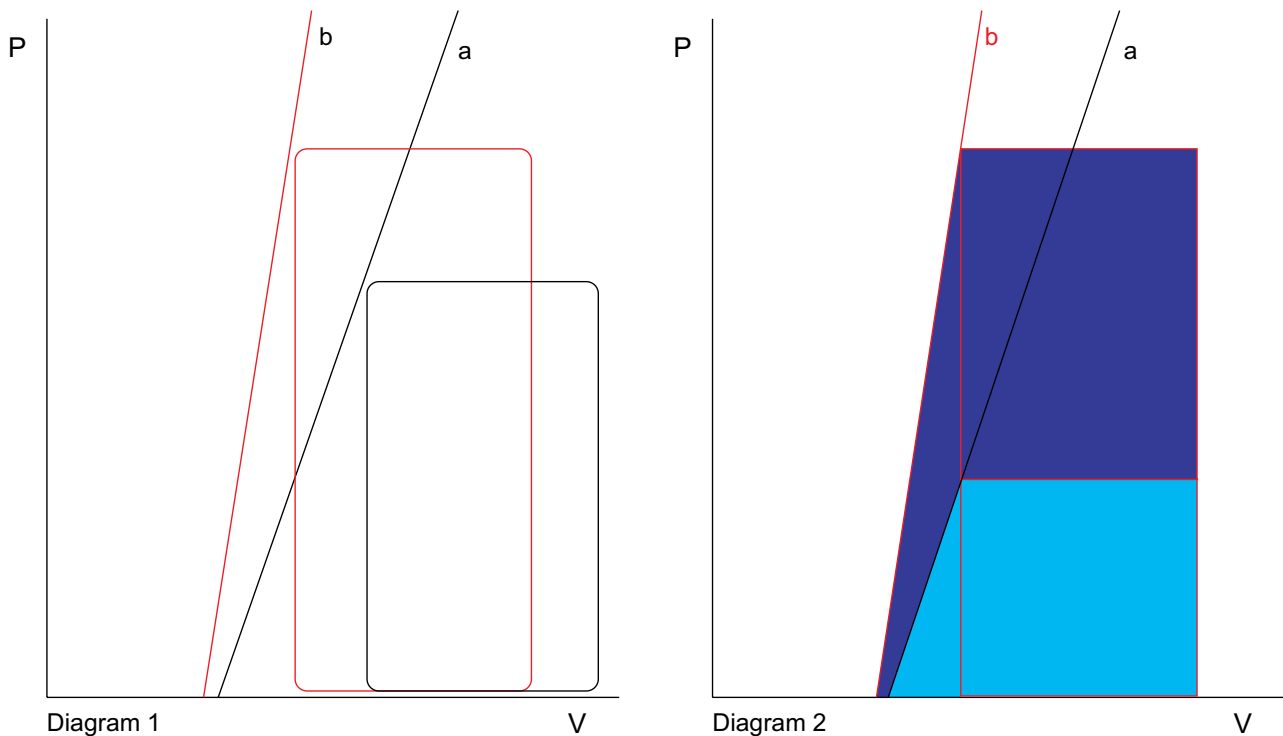


Figure 17. Diagram 1 is the pressure-volume curve of the heart (black box) and of the heart during direct cardiac compression (DCC, red box). Lines a and b represent the end systolic pressure volume relationship (ESPVR) of the heart and of the heart during DCC, respectively. The increased slope of the ESPVR during DCC demonstrates the increased contractility. Diagram 2 shows that the pressure volume area (PVA) of the heart during DCC, i.e. the total mechanical energy, consists of two parts: the PVA of the heart (light blue) and the PVA of the device (dark blue). The myocardial oxygen consumption is proportional to the PVA of the heart. So, comparing the two diagrams, it is clear that DCC reduces myocardial oxygen consumption.

with the ECG. The cardiac output could be monitored using the Doppler effect and the oxygen saturation using a simple pulse oximeter. With this information, the device's microcontroller will constantly know when the heart is going to contract, how much blood is actually flowing into the aorta, and whether there is hypoxemia. Based on all this incoming information the microcontroller can adjust the contraction of the artificial myocardium.

Current shaping (CS) and the DC are the means by which the microcontroller can adjust the contraction of the artificial myocardium, i.e. the velocity of the contraction, the duration of the contraction and the strain. Without CS and DC the operation of the artificial myocardium would be unsystematic. Up to now, of course, there is no clinical experience of controlling an artificial myocardium with CS and DC, but the effect of the artificial myocardium's velocity on the cardiac wall velocity will most probably be beneficial, since there is a strong positive correlation between pathological situations and pathological velocities. Lastly, using CS it might be proven in the future that assisting the heart through only a portion of its contraction could satisfactorily increase the cardiac output.

It was easily confirmed in the lab, using CS, that electrical currents of intensities higher than the manufacturer recommends (nominal value) can flow through the SMA fibers for short durations without destroying these fibers. It seems safe to exceed the nominal values with CS but for a very short duration.

The power of a healthy heart is around 1.3 to 2 watts,¹⁹ whereas that of a failing heart is much less, but not zero since there is blood flow. The artificial myocardium's power will be added to the power of the failing heart, thus assisting the circulation, not taking it over. The combined function of the native and artificial myocardia will restore the blood flow to normal levels. The ratio of this contribution could be adjusted. During moderate physical activities the contribution of the artificial myocardium could be automatically increased and if the heart recovers, this contribution could be decreased.

The partial or total recovery of a failing heart assisted by an MCS device is a possible scenario that is usually related to the phenomenon of reverse remodeling. This possibility is probably promoted by the increased myocardial perfusion that accompanies the use of these devices. In the case of total recovery, the explantation of the artificial myocardium could be optional. The artificial myocardium could be left inside the body in a standby mode in case it becomes

necessary again. The small volume of the device would cause no problems.

The relaxation of the fibers is a passive procedure. Similarly, the relaxation of the myocardium is also passive, even though there are some objections.²⁰ In the case where the cardiac walls relax earlier than the artificial myocardium there is the concern that this velocity discrepancy could have a detrimental effect on the treatment, perhaps causing cardiac tamponade. During diastole, the microcontroller will interrupt the current flow through the fibers, since the artificial myocardium's contraction will be synchronized with the ECG (possibly the P wave or the R wave). So the fibers will not exert any force during diastole, namely they will not actively impede the heart's relaxation. The relaxation of these fibers is rapid and their resistance to the cardiac wall's relaxation would be insignificant. Furthermore, the inelastic components of the artificial myocardium device will neither permit the progression of cardiac dilation nor the overstretching of the fibers. Thus, the artificial myocardium would promote the reverse remodeling of the heart.

In conclusion, the perspective of an MCS device characterized by small size and weight, great reliability, lack of any mechanical motor, lack of blood-contacting artificial surface, pulsatile flow, promotion of reverse remodeling and possible recovery, is the motive for the development of artificial myocardium. More studies need to be conducted in this direction. The final goal is to develop devices that would offer an equal or superior solution to heart transplantation.

Acknowledgement

The authors wish to thank Mr. Ioannis Koutsaidis for his valuable technical assistance.

References

1. Frazier OH, Myers TJ, Radovancević B. The HeartMate left ventricular assist system. Overview and 12-year experience. *Tex Heart Inst J.* 1998; 25: 265-271.
2. LePrince P, Bonnet N, Rama A, et al. Bridge to transplantation with the Jarvik-7 (CardioWest) total artificial heart: a single-center 15-year experience. *J Heart Lung Transplant.* 2003; 22: 1296-1303.
3. Moon YS, Ohtsubo S, Gomez MR, Moon JK, Nosé Y. Comparison of centrifugal and roller pump hemolysis rates at low flow. *Artif Organs.* 1996; 20: 579-581.
4. Copeland JG 3rd, Arabia FA, Banchy ME, et al. The CardioWest total artificial heart bridge to transplantation: 1993 to 1996 national trial. *Ann Thorac Surg.* 1998; 66: 1662-1669.

5. Shiraishi Y, Yambe T, Saijo Y, et al. Morphological approach for the functional improvement of an artificial myocardial assist device using shape memory alloy fibres. Proceedings of the 29th Annual International Conference of the IEEE EMBS Cité Internationale, Lyon, France, August 23-26, 2007.
6. Wang Q, Yambe T, Shiraishi Y, et al. Non-blood contacting electro-hydraulic artificial myocardium (EHAM) improves the myocardial tissue perfusion. *Technol Health Care*. 2005; 13: 229-234.
7. Kung RT, Rosenberg M. Heart booster: a pericardial support device. *Ann Thorac Surg*. 1999; 68: 764-767.
8. Kawaguchi O, Goto Y, Ohgoshi Y, Yaku H, Murase M, Suga H. Dynamic cardiac compression improves contractile efficiency of the heart. *J Thorac Cardiovasc Surg*. 1997; 113: 923-931.
9. Wang Q, Yambe T, Shiraishi Y, et al. An artificial myocardium assist system: electrohydraulic ventricular actuation improves myocardial tissue perfusion in goats. *Artif Organs*. 2004; 28: 853-857.
10. Chachques JC, Jegaden OJ, Bors V, et al. Heart transplantation following cardiomyoplasty: a biological bridge. *Eur J Cardiothorac Surg*. 2008; 33: 685-690.
11. Rubino AS, Onorati F, Santarpino G, et al. Neurohormonal and echocardiographic results after CorCap and mitral annuloplasty for dilated cardiomyopathy. *Ann Thorac Surg*. 2009; 88: 719-725.
12. Frazier OH, Gemmato C, Myers TJ, et al. Initial clinical experience with the HeartMate II axial-flow left ventricular assist device. *Tex Heart Inst J*. 2007; 34: 275-281.
13. Shiraishi Y, Yambe T, Sekine K, et al. Development of an artificial myocardium using a covalent shape-memory alloy fiber and its cardiovascular diagnostic response. Proceedings of the 2005 IEEE Engineering in Medicine and Biology 27th Annual Conference, Shanghai, China, September 1-4, 2005.
14. Karwatowski SP, Mohiaddin RH, Yang GZ, Firmin DN, St John Sutton M, Underwood SR. Regional myocardial velocity imaged by magnetic resonance in patients with ischaemic heart disease. *Br Heart J*. 1994; 72: 332-338.
15. Paraskos JA, Grossman W, Saltz S, Dalen JE, Dexter L. A non-invasive technique for the determination of velocity of circumferential fiber shortening in man. *Circ Res*. 1971; 29: 610-615.
16. Gault JH, Ross J Jr, Braunwald E. Contractile state of the left ventricle in man: instantaneous tension-velocity-length relations in patients with and without disease of the left ventricular myocardium. *Circ Res*. 1968; 22: 451-463.
17. Carlsson M, Ugander M, Heiberg E, Arheden H. The quantitative relationship between longitudinal and radial function in left, right, and total heart pumping in humans. *Am J Physiol Heart Circ Physiol*. 2007; 293: H636-644.
18. Kawaguchi O, Goto Y, Ohgoshi Y, Yaku H, Murase M, Suga H. Dynamic cardiac compression improves contractile efficiency of the heart. *J Thorac Cardiovasc Surg*. 1997; 113: 923-931.
19. Fay J, Sonwalkar N. *A Fluid Mechanics Hypercourse* [CD-ROM]. Cambridge, MA, MIT Press, 1996.
20. Buckberg GD. Basic science review: the helix and the heart. *J Thorac Cardiovasc Surg*. 2002; 124: 863-883.